PHYSICAL REVIEW A **86**, 050303(R) (2012)

Implementing one-photon three-qubit quantum gates using spatial light modulators

A. F. Abouraddy,[1,*] G. Di Giuseppe,[1,2] T. M. Yarnall,[3,†] M. C. Teich,[1,4] and B. E. A. Saleh[1]

[1]*CREOL, The College of Optics & Photonics, University of Central Florida, Orlando, Florida 32816, USA*

[2]*School of Science and Technology, Physics Division, University of Camerino, 62032 Camerino, Italy*

[3]*19 Chestnut Circle, Merrimack, New Hampshire 03054, USA*

[4]*Departments of Electrical & Computer Engineering and Physics, Boston University, Boston, Massachusetts 02215, USA*

(Received 20 July 2012; published 8 November 2012)

Increasing the information-carrying capacity of a single photon may be achieved by utilizing multiple degrees of freedom. We describe here an approach that utilizes two degrees of freedom to encode three qubits per photon: one in polarization and two in the spatial-parity symmetry of the transverse field. In this conception, a polarization-sensitive spatial light modulator corresponds to a three-qubit controlled-unitary gate with one control qubit (polarization) and two target (spatial-parity-symmetry) qubits. We describe the construction of controlled-NOT (CNOT), $\sqrt[n]{\text{CNOT}}$, controlled-PHASE, and Fredkin gates, and the preparation of one-photon, three-qubit Greenberger-Horne-Zeilinger (GHZ) and W states. This approach enables simple optical implementations of few-qubit tasks in quantum information processing.

DOI: 10.1103/PhysRevA.86.050303 PACS number(s): 03.67.Bg, 42.65.Lm, 03.67.Mn

Introduction. The most utilized realization of a photonic qubit is polarization. Increasing the information-carrying capacity of a photon requires making use of other degrees of freedom, such as orbital angular momentum (OAM) [1], discrete paths [2], spatial positions [3], time bins [4], frequency combs [5], or combinations thereof [6]. We have recently demonstrated [7–9] an alternative realization of a photonic qubit that relies on a global spatial symmetry: the parity symmetry of the transverse photon field. One qubit may be encoded per transverse field dimension [10], thus allowing two logical qubits to be encoded in a one-photon (1P) field *without* spatial or modal filtering. Simple optical devices implement one- and two-qubit operations on the parity-symmetry Hilbert space. Moreover, entangled parity-symmetry qubits may be encoded in photon pairs produced by spontaneous parametric downconversion [11], leading to the first violation of Bell's inequality using an Einstein-Podolsky-Rosen state [7,8].

In this Rapid Communication we investigate the utilization of polarization *in conjunction* with two-dimensional (2D) parity symmetry in 1P fields. In this conception, 1P states encode *three* logical qubits: two in the x- and y-parity symmetry and the third in polarization. We show that a polarization-sensitive spatial light modulator (PS-SLM) corresponds to a three-qubit controlled-unitary gate that couples spatial parity and polarization. While the usefulness of spatial light modulators (SLMs) in quantum optics is now appreciated for spatially modulating a photon wave front, typically in order to manipulate the orbital angular momentum content [12], the coupling between spatial and polarization degrees of freedom engendered by PS-SLMs has *not* heretofore been recognized. A PS-SLM corresponds in one configuration to a three-qubit controlled-NOT (CNOT) gate between polarization (control qubit) and spatial parity (two target qubits), and may also be configured to implement $\sqrt[n]{\text{CNOT}}$ gates. Using this device, a wide range of 1P three-qubit states may be prepared. Furthermore, the role of polarization and parity may be reversed. Our approach potentially enables simple implementations of quantum information processing protocols, and may also be extended to entangled multiphoton states.

One-qubit parity-symmetry operators. Consider a 1P state $|\Psi\rangle = \int dx\,\psi(x)|1_x\rangle$ with $\psi(x) = \alpha u_e(x) + \beta u_o(x)$, where $u_e(x)$ and $u_o(x) = h(x)u_e(x)$ are *even* and *odd* functions, respectively, and $h(x) = \text{sgn}(x)$ is the unit sign function. We map this class of states to the qubit $|\Psi\rangle = \alpha|e\rangle + \beta|o\rangle$ by associating the basis $\{|e\rangle,|o\rangle\}$ with the orthonormal functions $\{u_e(x),u_o(x)\}$ [7]. Simple optical transformations implement one-qubit logical operators. (1) Introducing a phase π between the two halves of the plane along x using a SLM corresponds to the Pauli operator $\hat{X}_x$. (2) Introducing a phase θ between the two halves of the plane corresponds to a parity rotation $\hat{R}_x(\theta) = \exp\{i\frac{\theta}{2}\hat{X}_x\}$ [Fig. 1(a)]. (3) A spatial reflection along x implemented with a dove prism, for example, corresponds to the Pauli operator $\hat{Z}_x$ [Fig. 1(b)]. (4) Projections $\hat{P}_x^e = \frac{1}{2}\{\hat{\mathbb{I}} + \hat{Z}_x\} = |e\rangle\langle e|$ and $\hat{P}_x^o = \frac{1}{2}\{\hat{\mathbb{I}} - \hat{Z}_x\} = |o\rangle\langle o|$ are implemented using a balanced Mach-Zehnder interferometer (MZI) with $\hat{Z}_x$ in one arm [Fig. 1(c)]. Similar devices, after appropriate rotations that exchange x for y, implement the corresponding operators on y-parity symmetry: $\hat{X}_y$, $\hat{R}_y(\theta)$, $\hat{Z}_y$, $\hat{P}_y^e$, and $\hat{P}_y^o$ [Figs. 1(d)–1(f)]. See Refs. [7,9,10] for details.

Two-qubit parity-symmetry operators. Two qubits are encoded per photon in the x and y transverse spatial dimensions. The 1P state $|\Psi\rangle = \iint dxdy\,\psi(x,y)|1_{x,y}\rangle$ with a state function of the form $\psi(x,y) = \sum_{i,j}\alpha_{ij}u_i(x)u_j(y)$, $i,j = e,o$, is mapped to the two-qubit state $|\Psi\rangle = \alpha_{ee}|ee\rangle + \alpha_{eo}|eo\rangle + \alpha_{oe}|oe\rangle + \alpha_{oo}|oo\rangle$. It is understood that $|ee\rangle = |e\rangle_x \otimes |e\rangle_y$, etc. By sculpting the spatial distribution of $\psi(x,y)$ an arbitrary 1P two-qubit state is prepared [10]. One- and two-qubit rotations are implemented in this 4D Hilbert space by modulating the phase of the four quadrants of the field in the x-y plane using a SLM [Figs. 1(g)–1(k)]. A phase modulation $\frac{\theta}{2}h(x)$ corresponds to the one-qubit operator $\hat{R}_x(\theta)\otimes\hat{I}_y$ which rotates the x-parity qubit [Fig. 1(g)]. The corresponding operator on y-parity symmetry, $\hat{I}_x \otimes \hat{R}_y(\theta)$, is implemented by the phase

*raddy@creol.ucf.edu

†Currently with Massachusetts Institute of Technology, Lincoln Laboratory, Lexington, MA 02420, USA.

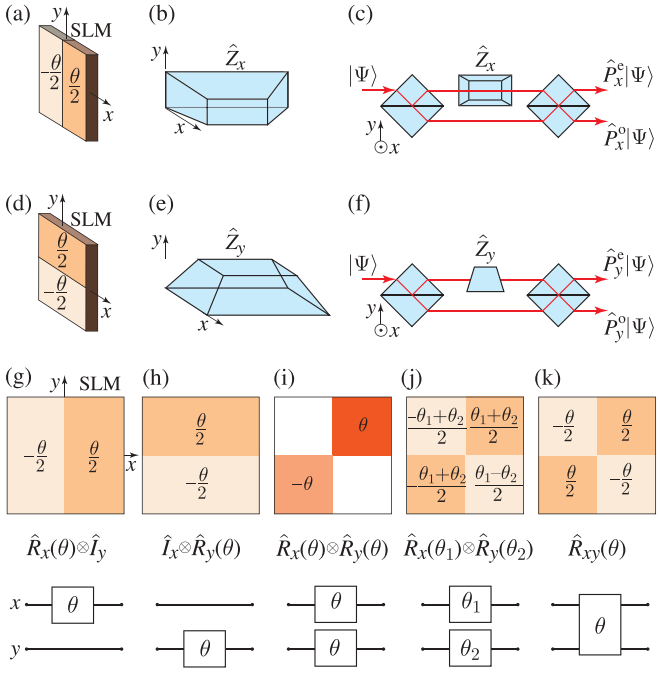

FIG. 1. (Color online) (a)–(c) x-parity-symmetry operators. (a) A SLM imparting a phase distribution $\frac{\theta}{2}h(x)$ corresponds to a parity-symmetry qubit rotation by an angle θ; (b) a dove prism that flips the field distribution along x corresponds to the Pauli $\hat{Z}_x$ operator; and (c) a balanced MZI with $\hat{Z}_x$ placed in one arm corresponds to a projection operator in the even-odd basis. (d)–(f) The y-parity-symmetry operators corresponding to (a)–(c). (g)–(k) Phase distributions in the x-y plane imparted by a SLM (black-bordered squares) to the transverse optical field in order to implement (g), (h) one-qubit and (i)–(k) two-qubit parity-symmetry rotation operators, and the corresponding quantum-circuit representations. Black lines correspond to 1D parity-symmetry qubits, and black boxes to rotation operators.

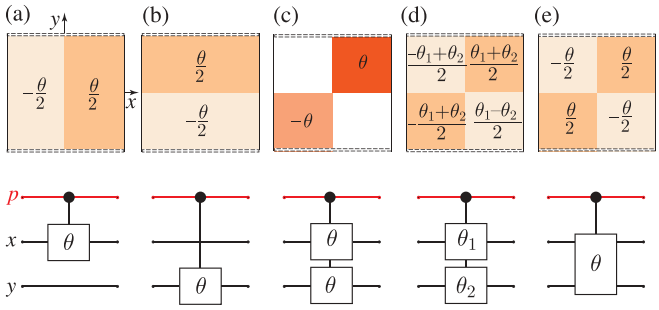

FIG. 2. (Color online) Phase distributions on a PS-SLM (with dashed bottom and top borders) to produce *controlled* one- and two-qubit rotation operators. (a) Controlled-$\hat{R}_x(\theta)$ or $\hat{\mathbb{C}}_x(\theta)$, (b) $\hat{\mathbb{C}}_y(\theta)$, (c) $\hat{\mathbb{C}}_x(\theta)\cdot\hat{\mathbb{C}}_y(\theta)$, (d) $\hat{\mathbb{C}}_x(\theta_1)\cdot\hat{\mathbb{C}}_y(\theta_2)$, and (e) $\hat{\mathbb{C}}_{xy}(\theta)$. In the corresponding quantum-circuit representations, the red (black) line corresponds to the polarization control (parity-symmetry target) qubit.

modulation $\frac{\theta}{2}h(y)$ [Fig. 1(h)]. These one-qubit operators may be combined by adding the corresponding phase distributions on one SLM. For example, $\hat{R}_x(\theta)\otimes\hat{R}_y(\theta)$, which rotates each parity qubit an angle θ, is implemented using the phase modulation $\frac{\theta}{2}\{h(x)+h(y)\}$ [Fig. 1(i)]. One may rotate each parity qubit a different angle, $\hat{R}_x(\theta_1)\otimes\hat{R}_y(\theta_2)$, using the phase modulation $\frac{\theta_1}{2}h(x)+\frac{\theta_2}{2}h(y)$ [Fig. 1(j)]. A rotation in the *joint* two-qubit space, $\hat{R}_{xy}(\theta)=\exp\{i\frac{\theta}{2}\hat{X}_x\otimes\hat{X}_y\}$, is implemented using the phase distribution $\frac{\theta}{2}h(x)h(y)$ [Fig. 1(k)] and results in entangling the two qubits: $\hat{R}_{xy}(\theta)|ee\rangle=c|ee\rangle+is|oo\rangle$, where $c=\cos\frac{\theta}{2}$ and $s=\sin\frac{\theta}{2}$. These operators commute and their *products* may thus be implemented using a single SLM by *adding* the corresponding phase distributions.

Finally, note that a spatial rotation by 90° in the x-y plane, thereby exchanging the x and y axes, corresponds to a two-qubit SWAP gate. Such a spatial rotation may be implemented using mirrors or an appropriate prism.

Three-qubit parity-polarization operators. Taking polarization now into consideration, *three* logical qubits are encoded in a 1P state: *two* in the spatial parity (x and y) and *one* in polarization. The 1P state space is now 8D and is the direct product of the 2D polarization space and the 4D-parity-symmetry space with basis $\{|H\rangle,|V\rangle\}\otimes\{|ee\rangle,|eo\rangle,|oe\rangle,|oo\rangle\}$. Besides increasing the information-carrying capacity of the photon, including polarization enables polarization-sensitive devices, such as a PS-SLM, to play the role of controlled-unitary gates. In particular, consider the phase distributions in Figs. 1(g)–1(k) when implemented by a PS-SLM that modulates *one* polarization component (say, $|H\rangle$, while $|V\rangle$ is unaffected); see Fig. 2. Imparting this phase modulation to the 2D wave front implements a *three-qubit polarization-controlled-unitary gate on the parity qubits*. Such a PS-SLM has in general the 8×8 matrix representation $\hat{\mathbb{C}}=\left(\begin{smallmatrix}\hat{R} & \hat{0}_4\\ \hat{0}_4 & \hat{I}_4\end{smallmatrix}\right)$, where $\hat{R}$ is a 4×4 2D-parity-symmetry unitary rotation (for $|H\rangle$ alone), and $\hat{I}_4$ and $\hat{0}_4$ are the 4D identity and zero operators, respectively. Polarization is the control qubit and the x- and y-parity symmetry are two target qubits. If the phase modulation on the PS-SLM is along x alone [Fig. 2(a)], then the resulting transformation is a controlled-unitary gate $\hat{\mathbb{C}}_x(\theta)$ on the x-parity qubit, similarly for a phase modulation on the PS-SLM along y alone, $\hat{\mathbb{C}}_y(\theta)$ [Fig. 2(b)]. Two independent one-qubit controlled-unitary rotations may be combined on the same PS-SLM: $\hat{\mathbb{C}}_x(\theta)\cdot\hat{\mathbb{C}}_y(\theta)$ [Fig. 2(c)] and $\hat{\mathbb{C}}_x(\theta_1)\cdot\hat{\mathbb{C}}_y(\theta_2)$ [Fig. 2(d)]. Finally, the phase modulation in Fig. 2(e) corresponds to a polarization-controllable two-qubit rotation by an angle θ, $\hat{\mathbb{C}}_{xy}(\theta)$. Moreover, such a gate may be dynamically reconfigured in real time by changing the encoded phase.

CNOT, CPHASE, and Fredkin gates. Several important quantum gates may be realized by setting specific values of rotation angles in these general controlled-unitary gates. For example, a CNOT gate corresponds to the special case of $\theta=\pi$. Therefore, a CNOT_x gate that operates on the x-parity-symmetry qubit is implemented using a PS-SLM imparting the phase modulation in Fig. 3(a). Similarly, a CNOT_y gate is implemented as shown in Fig. 3(b). CNOT_x and CNOT_y gates may be implemented simultaneously using a single PS-SLM [Fig. 3(c)]. It is important to stress the simplicity of constructing such gates which require only encoding the appropriate phase distributions on the PS-SLM.

Other quantum gates may be similarly implemented. For example, $\sqrt{\text{CNOT}_x}$, $\sqrt{\text{CNOT}_y}$, $\sqrt{\text{CNOT}_x}\cdot\sqrt{\text{CNOT}_y}$ [Fig. 3(d)] correspond to setting $\theta=\frac{\pi}{2}$ in the phase distributions in

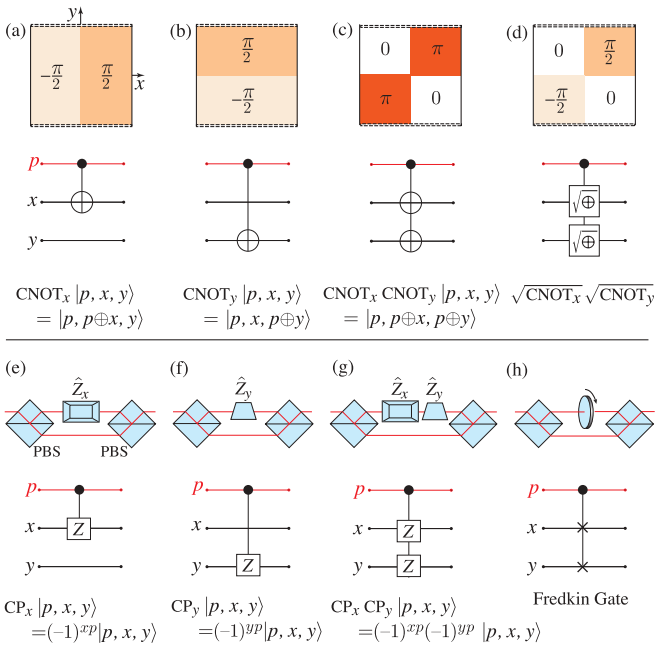

FIG. 3. (Color online) Three-qubit quantum gates. (a) CNOT_x, (b) CNOT_y, (c) the cascade $\mathrm{CNOT}_x \cdot \mathrm{CNOT}_y$, and (d) $\sqrt{\mathrm{CNOT}_x} \cdot \sqrt{\mathrm{CNOT}_y}$ gates, each implemented using a PS-SLM with the shown phase distribution. (e)–(g) Controlled-PHASE (CP) gates. PBS: polarizing beam splitter. The upper and lower paths in the MZI correspond to $|H\rangle$ and $|V\rangle$ polarization components, respectively. Z refers to the appropriate Pauli-Z operator acting on x or y parity. (h) A controlled-SWAP gate, or a quantum Fredkin gate.

Figs. 2(a)–2(c), respectively. A $\sqrt[n]{\mathrm{CNOT}}$ gate is implemented by setting $\theta = \frac{\pi}{n}$.

One- and two-qubit controlled-PHASE (CP) gates may also be constructed on the joint polarization and parity-symmetry space, as shown in Figs. 3(e)–3(g). Finally, in Fig. 3(h) we show an implementation of a Fredkin gate, a controlled-SWAP gate, using a balanced MZI that employs two polarizing beam splitters and a SWAP gate (a 90° spatial rotation) placed in one arm.

Generating one-photon three-qubit entangled states. Within this framework, a wide variety of three-qubit states may be prepared using simple optical arrangements (Fig. 4). We start from a separable state $|\Psi_1\rangle = |Hee\rangle$ [Fig. 4(a)]. As a first example, we entangle the two parity qubits while keeping the polarization qubit independent, thus producing the state $\frac{1}{\sqrt{2}}|H\rangle\{|ee\rangle + i|oo\rangle\}$ [Fig. 4(b)] using an SLM imparting the phase distribution in Fig. 1(k) with $\theta = \frac{\pi}{2}$, corresponding to $\hat{R}_{xy}(\frac{\pi}{2})$. Alternatively, one may entangle x parity (y parity) with polarization (Fig. 4(c) [Fig. 4(d)]), by rotating the polarization qubit with a half-wave plate (HWP), $|H\rangle \rightarrow \frac{1}{\sqrt{2}}\{|H\rangle + |V\rangle\}$, followed by a CNOT_x (CNOT_y) gate.

These examples correspond to states featuring *two-qubit* entanglement and a separable third qubit. It is well known that there are two families of genuine *three-qubit* entanglement: Greenberger-Horne-Zeilinger (GHZ) and W states [13]. 1P three-qubit GHZ and W states are readily prepared from $|Hee\rangle$, as shown in Figs. 4(e) and 4(f), respectively. The GHZ state $\frac{1}{\sqrt{2}}\{-|Hoo\rangle + |Vee\rangle\}$ is prepared by rotating the

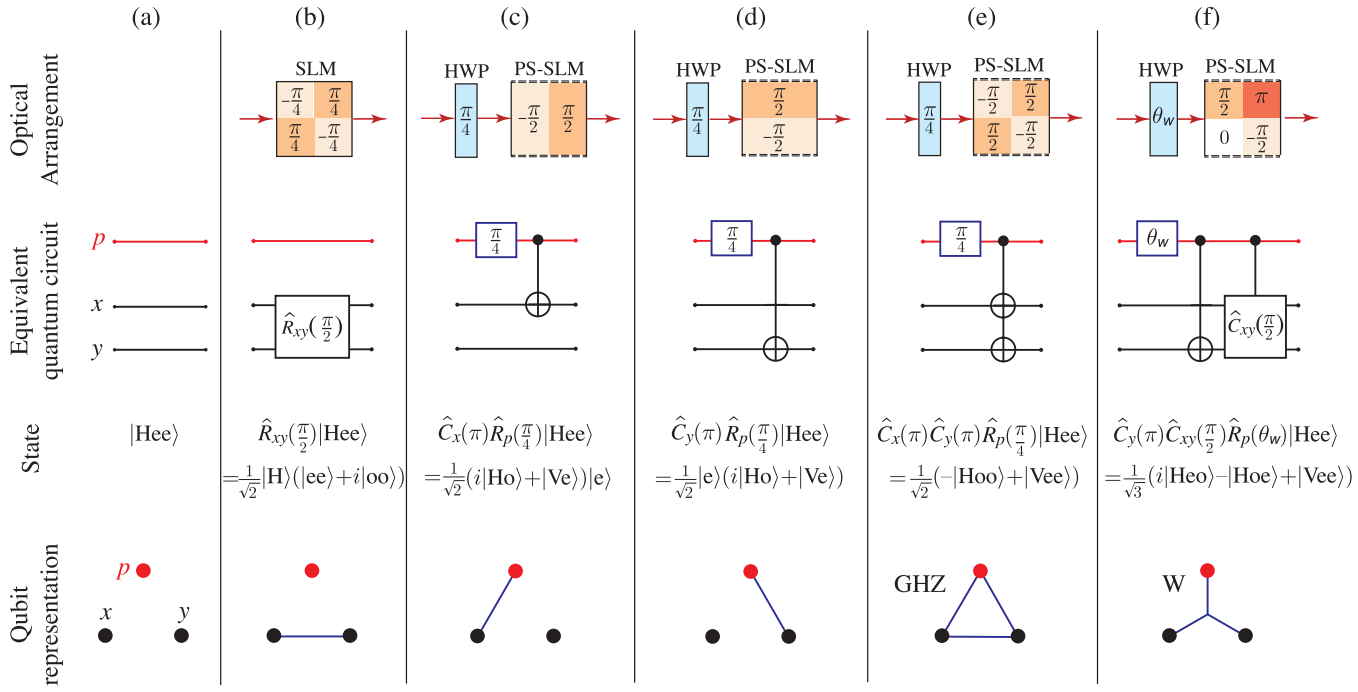

FIG. 4. (Color online) Preparing one-photon three-qubit entangled states. HWP: half-wave plate rotating $|H\rangle$ by ϕ: $\hat{R}_p(\phi)|H\rangle = \cos\phi|H\rangle + \sin\phi|V\rangle$; SLM: spatial light modulator (square with black boundary); PS-SLM: polarization-sensitive SLM (square with dashed bottom and top black boundary). The top row shows schematics of the optical arrangements to prepare the desired states starting from $|\Psi_1\rangle = |Hee\rangle$. The second row depicts the corresponding quantum circuit; the red line represents the polarization qubit and the black lines represent the x- and y-parity-symmetry qubits. The third row lists the prepared quantum state and the last row shows a pictorial representation of the state. Each qubit is represented by a circle (red for polarization, black for parity) and the blue lines represent entanglement between the connected qubits.

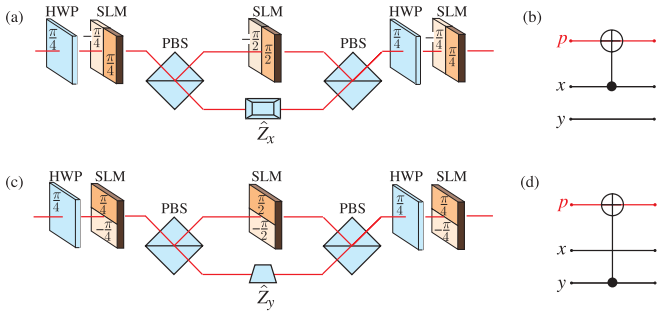

FIG. 5. (Color online) (a) Schematic of an optical arrangement to implement a CNOT gate with a control x-parity-symmetry qubit and a target polarization qubit and (b) the equivalent quantum circuit. (c), (d) Corresponding implementation and circuit for y-parity-symmetry control qubit.

polarization $\frac{\pi}{4}$ followed by a $\mathrm{CNOT}_x \cdot \mathrm{CNOT}_y$ gate. The W state $\frac{1}{\sqrt{3}}\{i|Heo\rangle - |Hoe\rangle + |Vee\rangle\}$ is prepared by rotating the polarization by $\theta_W = \tan^{-1}\frac{1}{\sqrt{2}}$ followed by a CNOT_y gate then $\hat{\mathbb{C}}_{xy}(\frac{\pi}{2})$. Since CNOT_y and $\hat{\mathbb{C}}_{xy}(\frac{\pi}{2})$ commute, they are implemented using a single PS-SLM [Fig. 4(f)]. The 1P three-qubit GHZ and W states cannot be converted into each other by unitary operators that affect polarization or parity alone.

Reversing the role of parity symmetry and polarization. A PS-SLM implements a controlled-unitary gate with the polarization qubit representing the control and the parity-symmetry qubits the target. The role of polarization and parity-symmetry qubits may be reversed, and a CNOT gate may be constructed with the x-parity-symmetry qubit the control and polarization the target. An example of one such implementation is shown in Fig. 5(a). The HWP rotates the $\{|H\rangle,|V\rangle\}$ basis to $\{\frac{1}{\sqrt{2}}(|H\rangle \pm |V\rangle)\}$. It is straightforward to confirm that the setup in Fig. 5(a) implements the transformation $|He\rangle \rightarrow |Ve\rangle, |Ho\rangle \rightarrow |Ho\rangle, |Ve\rangle \rightarrow |He\rangle, |Vo\rangle \rightarrow |Vo\rangle$. In other words, $|p,x\rangle \rightarrow |p \oplus x, x\rangle$, which is a CNOT gate with x-parity symmetry the control and polarization the target. A similar arrangement may be implemented, $|p,y\rangle \rightarrow |p \oplus y, y\rangle$, by rotating the SLMs by 90° and exchanging $\hat{Z}_x$ for $\hat{Z}_y$ [Fig. 5(c)]. The construction of further gates is facilitated using such a gate. For example, a two-qubit SWAP gate between x parity and polarization may be constructed by adding two CNOT_x gates [polarization control, x-parity target, Fig. 2(a)] to the gate in Fig. 5(a), one preceding it and one following it.

Implementation. Spatial-parity symmetry is a propagation *invariant* as a result of the even parity of the free-space-propagation operator. This relaxes constraints on placement of components in the optical arrangement. For example, the optical paths in the experiments reported in Refs. [8,9] extended for ∼2 m with optical components manipulating the parity symmetry along this length.

Two limitations to the performance of these gates arise from the SLM's: the effects of the "edges" between domains of constant phase and the precision of phase selection. We estimate the reduction in gate fidelity using current SLMs to be ∼1%–2%, which may be reduced via technical improvements. The main limitation in parity-symmetry experiments is the stability of the modified MZIs [Figs. 1(c)–1(f)] used for state projection. In Ref. [8] we achieve 91% visibility limited chiefly by alignment.

While optical realizations of CNOT gates have been realized [14], reports of implementations of fractional gates, such as $\sqrt{\mathrm{CNOT}}$, are lacking. Furthermore, since we use the full optical field with no spatial discretization, cascading multiple gates is straightforward. Moreover, by applying our approach to photon pairs produced by SPDC, two-photon six-qubit states may be prepared and sophisticated forms of hyperentanglement [15] may be explored. Finally, our approach may be applied to other spatial degrees of freedom, such as OAM [1]. In that case, a PS-SLM implements a controlled-unitary gate with polarization the control and OAM the target.

In conclusion, we have described an approach to encoding three qubits in one-photon states. Two qubits are encoded in the global spatial-parity symmetry of the 1P transverse field distribution and the third in its polarization. Simple optical components implement three-qubit controlled-unitary gates with either polarization or parity symmetry playing the role of control. Multiple gates may be readily cascaded, thereby paving the way to convenient implementations of few-qubit quantum information processing algorithms.

[1] A. Mair, A. Vaziri, G. Weihs, and A. Zeilinger, Nature (London) **412**, 313 (2001).

[2] J. G. Rarity and P. R. Tapster, Phys. Rev. Lett. **64**, 2495 (1990); G. Weihs, M. Reck, H. Weinfurter, and A. Zeilinger, Phys. Rev. A **54**, 893 (1996); A. Rossi, G. Vallone, A. Chiuri, F. De Martini, and P. Mataloni, Phys. Rev. Lett. **102**, 153902 (2009); A. Peruzzo *et al.*, Nat. Commun. **2**, 224 (2011).

[3] M. Fiorentino and F. N. C. Wong, Phys. Rev. Lett. **93**, 070502 (2004); M. Fiorentino, T. Kim, and F. N. C. Wong, Phys. Rev. A **72**, 012318 (2005); L. Neves *et al.*, Phys. Rev. Lett. **94**, 100501 (2005); M. N. O'Sullivan-Hale, I. A. Khan, R. W. Boyd, and J. C. Howell, *ibid.* **94**, 220501 (2005); S. P. Walborn, D. S. Lemelle, M. P. Almeida, and P. H. Souto Ribeiro, *ibid.* **96**, 090501 (2006).

[4] I. Ali-Khan, C. J. Broadbent, and J. C. Howell, Phys. Rev. Lett. **98**, 060503 (2007).

[5] N. C. Menicucci, S. T. Flammia, and O. Pfister, Phys. Rev. Lett. **101**, 130501 (2008); M. Pysher, Y. Miwa, R. Shahrokhshahi, R. Bloomer, and O. Pfister, *ibid.* **107**, 030505 (2011).

[6] J. T. Barreiro, N. K. Langford, N. A. Peters, and P. G. Kwiat, Phys. Rev. Lett. **95**, 260501 (2005).

[7] A. F. Abouraddy, T. Yarnall, B. E. A. Saleh, and M. C. Teich, Phys. Rev. A **75**, 052114 (2007).

[8] T. Yarnall, A. F. Abouraddy, B. E. A. Saleh, and M. C. Teich, Phys. Rev. Lett. **99**, 170408 (2007).

[9] T. Yarnall, A. F. Abouraddy, B. E. A. Saleh, and M. C. Teich, Phys. Rev. Lett. **99**, 250502 (2007); Opt. Express **16**, 7634 (2008).

[10] A. F. Abouraddy, T. M. Yarnall, G. Di Giuseppe, M. C. Teich, and B. E. A. Saleh, Phys. Rev. A **85**, 062317 (2012).

[11] B. E. A. Saleh, A. F. Abouraddy, A. V. Sergienko, and M. C. Teich, Phys. Rev. A **62**, 043816 (2000).

[12] E. Yao *et al.*, Opt. Express **14**, 13089 (2006); M. Stütz, S. Gröblacher, T. Jennewein, and A. Zeilinger, Appl. Phys. Lett. **90**, 261114 (2007); J. Leach *et al.*, Opt. Express **17**, 8287 (2009); W. M. Pimenta *et al.*, *ibid.* **18**, 24423 (2010).

[13] W. Dür, G. Vidal, and J. I. Cirac, Phys. Rev. A **62**, 062314 (2000).

[14] J. L. O'Brien, A. Furusawa, and J. Vučković, Nat. Photonics **3**, 687 (2009).

[15] A. F. Abouraddy, G. Di Giuseppe, T. M. Yarnall, M. C. Teich, and B. E. A. Saleh (unpublished).